

## Surface water-groundwater interface geomorphology leads to scaling of residence times

M. Bayani Cardenas<sup>1</sup>

Received 26 February 2008; revised 17 March 2008; accepted 20 March 2008; published 17 April 2008.

[1] We know little regarding how geomorphological features along the surface-groundwater interface collectively affect water quality and quantity. Simulations of surface water-groundwater exchange at increasing scales across bed forms, bars and bends, and basins show that groundwater has a power-law transit time distribution through all these features, providing a purely mechanistic foundation and explanation for temporal fractal stream chemistry. Power-law residence time distributions are almost always attributed to spatial variability in subsurface transport properties- something we show is not necessary. Since the different geomorphological features considered here are typical of most landscapes, fractal stream chemistry may be universal and is a natural consequence of water exchange across multifaceted interfaces. **Citation:** Cardenas, M. B. (2008), Surface water-groundwater interface geomorphology leads to scaling of residence times, *Geophys. Res. Lett.*, 35, L08402, doi:10.1029/2008GL033753.

### 1. Introduction

[2] Recent continuous long-term observations of stream water quality show fractal behavior across time-scales of decades [Kirchner *et al.*, 2000] implying a power-law residence time distribution (PLRTD) for water contributing solutes to streams. Solute traveling through watersheds, including the subsurface, may initially be flushed out rapidly but leave behind a persistent low-level tail. Subsurface hydrologists typically attribute PLRTDs to spatial variability in subsurface properties [Berkowitz *et al.*, 2006]. A continuous time random walk framework with appropriate event time distributions or with the combined effects of multi-rate mass transfer from immobile zones can capture heavy-tailing behavior but does not offer a detailed perspective on the physical mechanisms [Scher *et al.*, 2002; Berkowitz *et al.*, 2006]. Fractal stream chemistry may be explained by a very large but probably unrealistic dispersivity, on the order of the domain length, in a transport equation for a hillslope [Kirchner *et al.*, 2001]. Previous explanations vary in how they parameterize processes not defined explicitly, and which are typically assumed to be occurring at a smaller scale than the level of the model. Although some state-of-the-art distributed integrated watershed models fail to reproduce fractal behavior in stream chemistry despite sophisticated

parameterization methods [Page *et al.*, 2007], recent work with fully-coupled groundwater and land surface models suggests that the unsaturated zone plays a role in generating fractal behavior [Kollet and Maxwell, 2008].

[3] Since most surface water bodies are an expression of the water table and since near-surface groundwater flow paths typically originate from and end at streams, fluvial processes are intimately tied to groundwater processes, and this connection contributes to stream chemistry. But streams integrate signals coming from the hillslope, from the channel network, from hyporheic and riparian zones, from the soil and even from deep regional aquifers (Figure 1). Breakthrough curves (BTCs) from in-stream solute injection follow a PLRTD [Haggerty *et al.*, 2002] suggesting that hyporheic exchange could partly explain fractal stream chemistry up to timescales of days; but this does not explain the fractal behavior up to decades. Long-term fractal behavior is reproduced by an integrated soil-groundwater-stream solute transport model with differential advection and mass transfer due to watershed-scale mobile and immobile zones [Lindgren *et al.*, 2004]. Yet there are hardly any observations on where, when and how immobile zones come about within a watershed, particularly those that explain fractal behavior from days to decades, highlighting a significant knowledge gap. We have shown previously that 2D Tóthian regional flow results in PLRTDs [Cardenas, 2007]. Wörman *et al.* [2007] also found similar behavior where an analytical solution for 3D fractal topography-driven groundwater flow results in PLRTDs from scales of meters to thousands of kilometers. At each scale, power-law tailing occurs over 2–4 orders of magnitude in time. Does this mean that the interface between surface and groundwater has to be a fractal or is there a fundamental landscape or geomorphologic unit that is driving this signal? In this manuscript, we present a simple yet meaningful mechanistic explanation, while minimizing abstractions in the flow and transport dynamics and build off our previous study [Cardenas, 2007]. We focus on 2D features, both horizontal and vertical.

[4] Figure 1 illustrates how groundwater exiting in streams is routed through the subsurface at nested scales. At the basin scale, topography drives regional flow from recharge to discharge areas such as streams (Figures 1b and 1d). At the channel-floodplain scale, dynamic river meander migration generates unconfined shallow alluvial aquifers where stream water can be temporarily transported through as groundwater (Figure 1a). Finally, intra-channel geomorphologic features such as bed forms and bars induce surface water-groundwater exchange (Figure 1c). We quantify the role of these ubiquitous

<sup>1</sup>Department of Geological Sciences, University of Texas at Austin, Austin, Texas, USA.

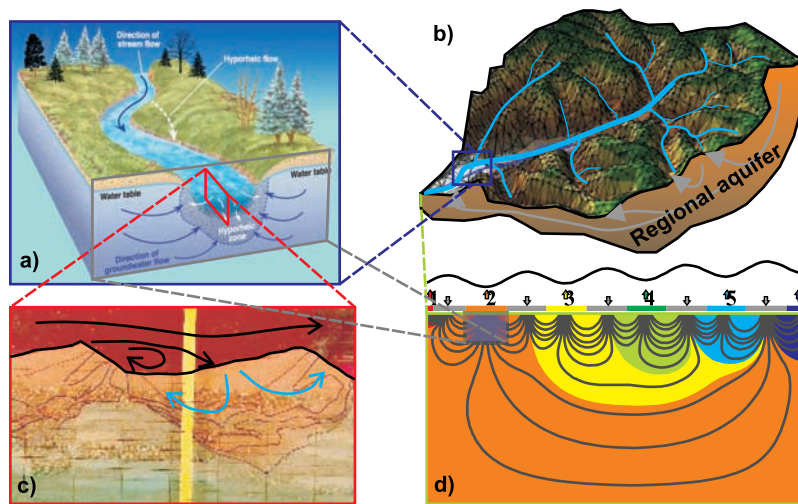


**Figure 1.** Conceptual picture of groundwater-surface water exchange across interfaces at nested scales. (a) Exchange across sinuous channel deposits and bars occurring at scales of meters to kilometers in some case [after *Alley et al.*, 2002], (b) diagram of a watershed [after *Ivanov et al.*, 2004], (c) vertical exchange due to in-channel features such as bars and bed forms with dimensions of centimeters to meters [after *Salehin et al.*, 2004], and (d) topography-driven regional exchange at kilometers to hundreds of kilometers [after *Cardenas*, 2007].

geomorphologic features in the generation of fractal stream chemistry.

## 2. Methods

[5] We numerically simulate flow and transport across bed forms, bars, and basins. The hydrodynamic model for flow through subaqueous dune sediment follows the method of *Cardenas and Wilson* [2007]. A numerical solution for turbulent stream flow over the dune is used to drive a groundwater flow model for the sediment. The turbulent flow model representing the vertically-two-dimensional river (as in Figure 1c) solves the steady-state Reynolds-averaged Navier-Stokes (RANS) equations and the  $k-\omega$  closure scheme [Wilcox, 1991]. The top of the turbulent flow domain, i.e., the river water surface, is a slip/symmetry boundary while the bottom, the sediment-water interface, is a no-slip boundary. The left and right boundaries are spatially periodic boundaries with a prescribed pressure drop resulting in flow from left to right of the domain, as in Figure 1c.

[6] The sediment or aquifer is governed by the groundwater flow equation:

$$\frac{\partial}{\partial x_i} \left( -\frac{k_p}{\mu} \frac{\partial P}{\partial x_i} \right) = 0 \quad (1)$$

where  $k_p$  is the permeability,  $\mu$  is the viscosity, and  $P$  is pressure; the parenthetical term is the Darcy flux. The pressure solution along the bottom of the turbulent flow model is used as a prescribed pressure boundary for the top of the groundwater flow domain effectively linking the two domains. The bottom of the sediment domain is a no-flow boundary and the left and right sides are spatially periodic boundaries with the same pressure drop prescribed in the turbulent flow model.

[7] Solute transport through the porous sediment and aquifers is modeled following the advection-diffusion-dispersion equation:

$$\frac{\partial C}{\partial t} = (D^m + D_{ij}) \frac{\partial^2 C}{\partial x_i^2} - \frac{q_i}{n} \frac{\partial C}{\partial x_i} \quad (2)$$

where  $C$  is concentration,  $t$  is time,  $n$  is porosity ( $=0.3$ ), and  $D^m$  is the molecular diffusion coefficient in porous media.  $D$ , the mechanical dispersion coefficient tensor is defined as follows:

$$D_{ij} = \alpha_T U \delta_{ij} + (\alpha_L - \alpha_T) u_i u_j / U \quad (3)$$

where  $\alpha_T$  and  $\alpha_L$  are transverse and longitudinal dispersivity,  $u$  is the pore velocity with magnitude  $U$ , and  $\delta_{ij}$  is the Kronecker delta function.  $\alpha_L$  is set at 0.1 cm typical for the scale of the dune sediment domain.  $\alpha_T$  is considered to be 1/10 of  $\alpha_L$ . In all simulations,  $D^m$  is set at  $5 \times 10^{-11} \text{ m}^2/\text{s}$  which is typical for geologic materials.

[8] Figure 2a shows our model triangular bed form which has a length of 1 m and whose crest is located at 0.8 m and is 0.05 m high. In the bed form case, the sediment-water interface is divided into solute in-flow and out-flow zones based on the distribution of Darcy velocity normal to the interface. The dividing point between these two zones corresponds to a “hinge-line” in the velocity distribution. The in-flow zone assumes a prescribed concentration following step injection, while the out-flow zones are convective boundaries. Permeability for the bed form is set at  $2 \times 10^{-10} \text{ m}^2$  corresponding to well-sorted coarse sand to gravel.

[9] The RANS- $k-\omega$  equations are numerically solved using the finite-volume approach as implemented in the code CFD-ACE+. The groundwater flow and solute transport equations are solved using the finite-element method implemented in COMSOL Multiphysics. Lagrange-

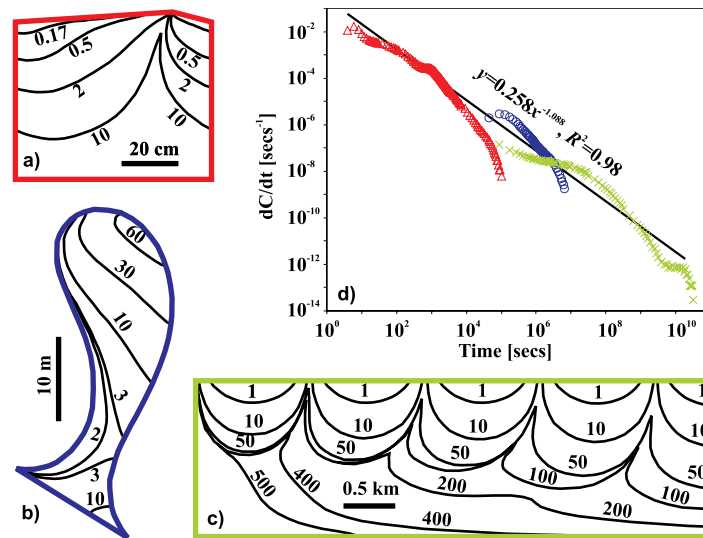


**Figure 2.** Solute fronts ( $C/C_0 = 0.5$ ) and residence time distributions for exchange at three scales. (a) Solute fronts for transport through a dune (front labels correspond to hours after solute release), (b) solute fronts for transport through a channel bend deposit (labels correspond to days after release), (c) solute fronts for transport at the watershed scale (labels correspond to years after release), and (d) breakthrough curve for all scales.

Quadratic triangular elements are used in COMSOL Multiphysics with node spacing less than 2 cm within the domain and less than 1 cm along the sediment-water interface for the bed form case.

[10] Groundwater flow and transport through a horizontally two-dimensional point bar (Figure 2b) and a vertically two-dimensional regional aquifer (Figure 2c) is similarly simulated via coupled finite-element solutions of equations (1)–(3) using COMSOL Multiphysics. The result from previous hydraulic-geomorphologic model of meandering channel evolution by *Boano et al.* [2006] (Figure 2b) is linearly scaled and used as input for meander geometry. The point bar model takes on a prescribed pressure boundary along the sinuous channel where the pressure varies linearly from the upstream end (left) to the downstream corner (right). A head gradient of 0.0001, typical of highly-sinuous low-gradient rivers, is imposed along the natural coordinate system representing the channel. The lower boundary (straight edge in Figure 2b) is a no-flow boundary. The zones where groundwater flow is into the point bar are considered as step-injection boundaries while discharge zones are convective boundaries. For the point bar case,  $\alpha_L = 1$  m,  $\alpha_T = 0.1\alpha_L$ , and  $k_p = 5.9 \times 10^{-11}$  m<sup>2</sup> (equivalent to a hydraulic conductivity of 50 m/d). The permeability is typical of fluvial deposits at the study scale while the dispersivities are on the conservative side to emphasize the role of the morphology-driven flow field, rather than local variability in aquifer properties. Maximum node spacing is 0.3 m within the domain and 0.1 m along the boundaries.

[11] We model basin-scale flow following *Cardenas* [2007], where the top boundary condition for equation (1) is a pressure distribution described by a harmonic function superposed on a linear gradient (i.e., Figure 1d) described by:

$$h(x_1, x_2 = 0) = mx_1 + h_{amp}[(\sin(\omega x_1))] \quad (4)$$

where  $h$  is head ( $= P/\rho g$ ),  $m$  is the regional head (or topographic) gradient,  $h_{amp}$  is the amplitude of the local fluctuations, and  $\omega = 2\pi/\lambda$  is the angular frequency, where  $\lambda$  is the wavelength of the fluctuations. We assume that  $m = 0.01$ ,  $h_{amp} = 50$  m, and  $\lambda = 1111$  m. The rectangular domain is 5 km  $\times$  1.5 km. The regional change in head and  $h_{amp}$  are small compared to the domain making a flat top boundary where the head undulations are imposed a suitable assumption [*Cardenas*, 2007]. For this regional 2D aquifer,  $\alpha_L = 100$  m,  $\alpha_T = 0.1\alpha_L$ , and  $k_p = 1.2 \times 10^{-12}$  m<sup>2</sup> (equivalent to a hydraulic conductivity of 1 m/d). The permeability is typical of basin-scale aquifers while the dispersivity is on the smaller side [*Ingebritsen and Sanford*, 1998], again to de-emphasize the role of dispersion. Boundary conditions for the in-flow and out-flow solute zones are similar to those in the dune and point bar cases. Maximum node spacing is 20 m within the domain and 5 m along the boundaries.

[12] The resulting solute breakthrough curves at the out-flow zones for all cases are flux weighted. For step-injection, the time-derivative of the breakthrough curves gives the residence time distributions (RTDs) for the solute, i.e., Figure 2d.

### 3. Results and Discussion

[13] The individual RTDs through all three geomorphic features at increasing spatial scales have power-law tails with slopes  $k$  of  $\sim -1.6$  to  $\sim -1.9$  (Figure 2d). A power-law RTD (PLRTD) with  $-2 \leq k \leq -1$  indicates an infinite residence time even though the transported entity is of finite amount [*Haggerty et al.*, 2000]. These tails are driven by differential advection due to multiple path lengths and variable head gradients which drives groundwater flow at different rates, including the development of stagnation zones. In all cases, no heterogeneity is considered in the transport properties of the sediments/aquifers although the effect of aquifer heterogeneity is included in the solute



transport via a conservative value for dispersivity at each scale. This is in stark contrast to the prevailing concept where RTDs, particularly non-Gaussian ones, are typically explained as resulting from geological heterogeneity.

[14] At the centimeter to meter bed form scale, both stagnation zones and infinitesimal path lengths at the hinge line between in-flow and out-flow zones are present within the same domain. This flow field is quite sensitive to the interaction between turbulent flow in the channel and the morphology of the bed form (see *Cardenas and Wilson* [2007] for a detailed discussion). Groundwater flow velocities are largest near the top of the bed forms where path lengths are shortest and smallest in areas penetrated by deeper paths mimicking extreme heterogeneity in hydraulic properties, i.e., mobile-immobile types of fields. This results in deceleration of a solute plume entering the sediments (Figure 2a). *Wörman et al.* [2007] have shown a similar behavior through a 3D riverbed that is considered to be flat but with a 3D variable pressure field. The pressure field is a fractal since it is a scaled replica of the topography which they have shown to be a fractal. It is unclear whether fractality in the bed form topography is necessary in order to get a PLRTD. We show that this is driven by exchange through a single bed form. Having a fractal field is not key, but perhaps serves to enhance this behavior. This RTD is expected in many instances where a fractal interface is not present at all but where such 2D features exist. The scaling of bed form geometry also suggests that although we analyze only one dune case here, the same hydrodynamic and residence time scaling would persist across scales where there is an approximately triangular bed form, even up to dunes whose lengths are tens of meters.

[15] A similar behavior persists at the watershed scale, except that this time the highly variable flow fields are nested [*Cardenas*, 2007]. This leads to a more pronounced power-law tail as some solutes are flushed through local flow cells while others are transported through deeper and longer paths (Figures 1d and 2c). However, similar nested flow fields are to be expected in river sediments since bed forms scale across space with multiple features such as ripples and dunes commonly superimposed [*Jerolmack and Mohrig*, 2005].

[16] A different scenario occurs in flow through point bar deposits of meandering channels where the groundwater flow is sinuosity-driven [*Boano et al.*, 2006]. The meander morphology, even at small sinuosity, produces a distribution of path lengths subjected to different head gradients [*Boano et al.*, 2006], again driving power-law behavior in the residence times (Figure 2d). *Wörman et al.* [2007] and *Cardenas* [2007] have shown how vertically oriented exchange across interfaces leads to PLRTDs. We now show that 2D horizontal exchange with river banks is also a fundamental contributor to fractal stream chemistry.

[17] Sinuous channels are typical of fluvial settings. Sand or gravel bars in channels attached to banks, to certain extent, are a smaller scale version of a point bar deposit. Even braided rivers are essentially a collection of meandering channels. The pervasiveness and known scale-invariance of channel bends with bars [*Stolum*, 1996] suggests that surface water-groundwater exchange through point bars will result in PLRTDs across broad time spans. But as in the bed form case, focusing on one meander shows that this funda-

mental geomorphologic feature by itself leads to PLRTD. Having several meanders across multiple scales emphasizes and prolong the effects of the PLRTD but the generation of the RTD occurs within an elementary unit.

[18] The RTDs by *Wörman et al.* [2007] were defined using particle-tracking unlike in our case where we numerically solve the advection-diffusion-dispersion equations for solutes (equation (2)). We do find similar patterns and behavior using another approach and are able to more clearly resolve the tails. There are salient differences between our methods. Here, we do not ignore the geomorphologic features at two scales- the bed forms and the point bar. Our simulations for the bed form scale is more complex than that by *Wörman et al.* [2007] in that we explicitly consider the processes in the turbulent channel as well and geometry of the bed form. Moreover, *Wörman et al.* [2007] have not analyzed the contributions of channel sinuosity to surface water-groundwater exchange- an important feature of the coupled system. Our 2D analysis for basins that follows *Cardenas* [2007] is basically the same as that by *Wörman et al.* [2007] where we both assume that the surface water-groundwater interface is flat while the topography is represented by a head distribution, but we consider only one-dimension and one one period/amplitude of the harmonic function (i.e., equation (4)). What we also show is that the interface topography, be it the bed form or the channel bend, need not have fractal geometry. A single feature is all that is needed to generate a PLRTD. But fractal scaling of a given geomorphologic feature serves to propagate this scaling more. But despite different representations of the complexity in the underlying physics and interfacial features, it is becoming clear that the geomorphology of the surface water-groundwater interface at all scales leads to PLRTDs.

[19] The effects of the geomorphological features on exchange flow and transport are ultimately integrated and a single curve can be fitted to the collective results. Unlike *Wörman et al.* [2007], we attempt to link the overlapping scales. In this case, the largest value for the time-derivative of the BTC is used when there is overlap (Figure 2d). The model outputs are not at exactly overlapping times disallowing direct superposition of the RTDs. Although each RTD has been flux-weighted, no additional weighting is done for the collective RTD effectively giving each scale's RTD equal weight. A power-law fit to the collective RTD results in  $k$  close to  $-1$  covering the range from a few seconds to myriad centuries (Figure 2d),  $\sim 10$  orders of magnitude in time, even much broader than that observed by *Kirchner et al.* [2000]. A slope equal to  $-1$  is unsustainable since this suggests that mass is not conserved, i.e., the zeroth moment of the RTD is infinite [*Haggerty et al.*, 2000]. This PLRTD would eventually drop off to a steeper slope or to an exponential behavior, which it does (Figure 2d). The individual RTDs corresponding to different scales all drop off eventually, but at some point transport at a larger spatial (and time) scale becomes pertinent. This allows for a persistent  $k$  close to  $-1$ . A finite mass released from the surface water-groundwater interface that does not return to the surface immediately following relatively short but distributed path lengths eventually joins a larger flow field also characterized by a distribution of path lengths and flow rates. Some mass transported at the bed form scale

eventually follow the flow fields at the point bar and then regional aquifer scale. From the perspective of a smaller nested flow system, the flow at the larger scale represents an “immobile” zone of infinite extent.

[20] Our analyses show that PLRTDs, and therefore fractal stream chemistry, can be driven solely by the geomorphological template of the surface water-groundwater interface. Heterogeneity in subsurface transport properties would only enhance this but keeping it to a minimum via conservative dispersivity values allows us to isolate the effects of geomorphology. In the past, spectral analysis of time-variant stream chemistry demonstrated a powerful “lumped” approach. But this presents more questions that are due to lack of direct knowledge of what the RTD through a coupled surface-subsurface watershed is and its genesis. Continuous-time random walk formulations and transport equations with mobile-immobile domains have provided a convenient foundation for modeling and interpreting PLRTDs, but the mechanistic basis for these is still not sufficiently clear. Our analysis with minimal abstraction of the flow and transport physics provides a more transparent picture and shows what signals are generated by geomorphological features. Since the features that we considered are found at most scales in most landscapes, power-law residence time distributions and fractal stream chemistry may be universal and is a natural consequence of groundwater-surface water exchange across ever-present yet spatially complex interfaces.

[21] **Acknowledgments.** This work was made possible through hardware and software support from the University of Texas at Austin Jackson School of Geosciences. Earlier versions of this manuscript benefitted from comments from John Hoaglund, George M. Hornberger, Donald I. Siegel and two anonymous reviewers.

## References

- Alley, W. M., R. W. Healy, J. W. Labaugh, and T. E. Reilly (2002), Flow and storage in groundwater systems, *Science*, *296*, 1985–1990.
- Berkowitz, B., A. Cortis, M. Dentz, and H. Scher (2006), Modeling non-Fickian transport in geological formations as a continuous time random walk, *Rev. Geophys.*, *44*, RG2003, doi:10.1029/2005RG000178.
- Boano, F., C. Camporeale, R. Revelli, and L. Ridolfi (2006), Sinuosity-driven hyporheic exchange in meandering rivers, *Geophys. Res. Lett.*, *33*, L18406, doi:10.1029/2006GL027630.
- Cardenas, M. B. (2007), Potential contribution of topography-driven regional groundwater flow to fractal stream chemistry: Residence time distribution analysis of Tóth flow, *Geophys. Res. Lett.*, *34*, L05403, doi:10.1029/2006GL029126.
- Cardenas, M. B., and J. L. Wilson (2007), Dunes, turbulent eddies, and interfacial exchange with permeable sediments, *Water Resour. Res.*, *43*, W08412, doi:10.1029/2006WR005787.
- Haggerty, R., S. A. McKenna, and L. C. Meigs (2000), On the late-time behavior of tracer test breakthrough curves, *Water Resour. Res.*, *36*(12), 3476–3479.
- Haggerty, R., S. M. Wondzell, and M. A. Johnson (2002), Power-law residence time distribution in the hyporheic zone of a 2nd-order mountain stream, *Geophys. Res. Lett.*, *29*(13), 1640, doi:10.1029/2002GL014743.
- Ingebritsen, S. E., and W. E. Sanford (1998), *Groundwater in Geologic Processes*, 341 pp., Cambridge Univ. Press, New York.
- Ivanov, V. Y., E. R. Vivoni, R. L. Bras, and D. Entekhabi (2004), Catchment hydrologic response with a fully distributed triangulated irregular network model, *Water Resour. Res.*, *40*, W11102, doi:10.1029/2004WR003218.
- Jerolmack, D. J., and D. Mohrig (2005), A unified model for subaqueous bed form dynamics, *Water Resour. Res.*, *41*, W12421, doi:10.1029/2005WR004329.
- Kirchner, J. W., X. Feng, and C. Neal (2000), Fractal stream chemistry and its implications for contaminant transport in catchments, *Nature*, *403*, 524–527.
- Kirchner, J. W., X. Feng, and C. Neal (2001), Catchment-scale advection and dispersion as a mechanism for fractal scaling in stream tracer concentrations, *J. Hydrol.*, *254*, 82–101.
- Kollet, S. J., and R. M. Maxwell (2008), Demonstrating fractal scaling of baseflow residence time distribution using a fully-coupled groundwater and land surface model, *Geophys. Res. Lett.*, *35*, L07402, doi:10.1029/2008GL033215.
- Lindgren, G. A., G. Destouni, and A. V. Miller (2004), Solute transport through the integrated groundwater-stream system of a catchment, *Water Resour. Res.*, *40*, W03511, doi:10.1029/2003WR002765.
- Page, T., K. J. Beven, J. Freer, and C. Neal (2007), Modeling the chloride signal at Plynlimon, Wales, using a modified dynamic TOPMODEL incorporating conservative chemical mixing (with uncertainty), *Hydrol. Processes*, *21*, 292–307.
- Salehin, M., A. I. Packman, and M. Paradis (2004), Hyporheic exchange with heterogeneous streambeds: Laboratory experiments and modeling, *Water Resour. Res.*, *40*, W11504, doi:10.1029/2003WR002567.
- Scher, H., G. Margolin, R. Metzler, J. Klafter, and B. Berkowitz (2002), The dynamical foundation of fractal stream chemistry: The origin of extremely long retention times, *Geophys. Res. Lett.*, *29*(5), 1061, doi:10.1029/2001GL014123.
- Stølum, H.-H. (1996), River meandering as a self-organization process, *Science*, *271*, 1710–1713.
- Wilcox, D. C. (1991), A half century historical review of the  $k-\omega$  model, paper AIAA-1991-615 presented at Aerospace Sciences Meeting, Am. Inst. of Aeronaut. and Astronaut., Reno, Nev.
- Wörman, A., A. I. Packman, L. Marklund, J. W. Harvey, and S. H. Stone (2007), Fractal topography and subsurface water flows from fluvial bed forms to the continental shield, *Geophys. Res. Lett.*, *34*, L07402, doi:10.1029/2007GL029426.

M. B. Cardenas, Department of Geological Sciences, University of Texas at Austin, Austin, TX 78712, USA. (cardenas@mail.utexas.edu)